New computational method in the theory of spinodal decomposition*

J. S. Langer†
Physics Department, Harvard University, Cambridge, Massachusetts 02138

M. Bar-on and Harold D. Miller
Carnegie-Mellon University, Pittsburgh, Pennsylvania 15213

(Received 5 December 1974)

We present a new series of calculations in the theory of spinodal decomposition. The computational scheme is based on a simple ansatz for the two-point distribution function which leads to closure of the hierarchy of equations of motion for the high-order correlation functions. The resulting theory is accurate throughout the spinodal region of the phase diagram, including at the boundaries of this region where the spinodal mechanism is difficult to distinguish from nucleation and growth. The computational scheme is worked out in detail for parameters approximating those of the three-dimensional, kinetic, spin-exchange Ising model with nearest-neighbor interactions. Numerical agreement with recent Monte Carlo data appears to be satisfactory.

I. INTRODUCTION

The term "spinodal decomposition"[1,2] refers to the initial stage of phase separation which occurs in a quenched, thermodynamically unstable, solid solution. Among the various kinetic mechanisms associated with first-order phase transformations, spinodal decomposition is distinguished from, say, nucleation and growth in that it requires no thermal activitation energy; that is, it occurs in the unstable rather than in the metastable region of a phase diagram. A second distinguishing characteristic is that the order parameter which describes the system, usually a composition variable, obeys a local conservation law. Thus the decomposition is limited by diffusionlike processes and, in its later stages, exhibits slow coarsening rather than the rapid approach to completion which occurs in magnetic or structural phase transformations. Also characteristic of the class of transformations to be considered here is that the process is assumed to occur isothermally. That is, each point in the system is assumed to be in strong contact with a heat reservoir, so that temperature fluctuations may be ignored and there is no constraint of local energy conservation.

The most common experimental examples of spinodal decomposition occur in metallic alloys[3,4] and glassy mixtures.[5-7] For example, an Al-rich Al-Zn alloy, when quenched rapidly from above 400°C and then annealed at temperatures in the neighborhood of 100°C, is known to decompose into Al- and Zn-rich regions via the spinodal mechanism.[3] A few other similar systems have been investigated; and recently there has begun to accumulate a small amount of accurate x-ray and electron-microscope data. As seen through the microscope, the reaction begins with the appearance of a fine, uniformly dispersed precipitate, which subsequently coarsens and develops into distinct regions of the equilibrium phases. It is probable that spinodal decomposition occurs in all alloy systems where there is a miscibility gap, but the mechanism may often be obscured by competing processes having to do with grain boundaries, dislocations, etc. A spinodal reaction has recently been observed in a two-component fluid,[8] but here the possibility of hydrodynamic effects must complicate the process, especially during coarsening. In principle, the spinodal mechanism should occur in condensation or solidification; however, the unstable spinodal states of pure fluids are experimentally inaccessible because one cannot quench rapidly enough to avoid initiating transformations via nucleation. Perhaps the most reliable "experimental" data to date are those obtained recently by computer simulation using the spin-exchange kinetic Ising model.[9,10] We shall refer to the latter model frequently throughout this paper.

The basic theory of spinodal decomposition has been developed, primarily from a metallurgical point of view by Hillert,[11,12] Cahn,[13,14] Hilliard,[2] and Cook.[15] The original work of Hillert[11,12] was a numerical investigation of a nonlinear, one-dimensional model. Subsequently, Cahn[13,14] developed a more general linearized theory of the spinodal instability. The role of thermal fluctuations was later described by Cook,[15] still within the linear approximation. Cahn, in an important paper,[16] pointed out the essential role played by nonlinear effects in determining the nature of the instability and then in limiting its growth, but Cahn did not attempt to formulate a statistical theory based on

his nonlinear equations. This latter project has subsequently been attempted by the present authors.[17-19] The underlying statistical formulation, along with a treatment of the later-stage coarsening problem, was presented in Ref. 17. References 18 and 19 were devoted to the development of approximate methods for solving the general master equation in Ref. 17.

In the present paper, we shall describe a new computational technique which refines and extends the methods introduced previously. Each of these previous methods had serious limitations which we believe are largely overcome by the new technique. Specifically, in using what we called the "mean-field" approximation,[19] we were limited to the very early stages of the spinodal reaction, that is, to the stages preceding the occurrence of any appreciable phase separation. On the other hand, the longer-time computations based on a phase-space cell analysis[18] gave the structure factor at only a few values of the wave vector, and thus were not really adequate for comparison with experiment. Both approximation schemes had the serious drawback of being unable to deal with the asymmetric nonlinear instability which occurs near the spinodal line (the classical limit of metastability) and whose importance has been emphasized by Cahn.[16]

Our main purpose throughout this project has been to develop a quantitative theory of spinodal decomposition which will be sufficiently accurate to be used with confidence in the analysis of a potentially rich body of experimental information, and which will, at the same time, be flexible enough to deal with real metallurgical effects not easily studied by computer simulation. We want eventually, for example, to study the effects of coherency stresses on the spinodal reaction. It might also be interesting to use the methods developed here to study the simultaneous phase separation and ordering which occurs near the tricritical point in the Fe-Al system.[20] Accordingly, the present paper is devoted to the description of a computational technique which we hope will be accurate throughout the spinodal region, and to the preliminary testing of this technique using parameters derived from the kinetic Ising model.

The scheme of this paper is as follows. In Sec. II, we summarize the underlying stochastic model and review briefly the linear and mean-field approximations. Section III contains a complete description of our new approximation scheme. Scaling aspects of this theory are discussed in Sec. IV. In Sec. V we consider a specific application of our theory to the kinetic Ising model. Section VI contains a summary and analysis of our numerical results, and Sec. VII is a brief review of our general conclusions.

II. SUMMARY DESCRIPTION OF THE MODEL

The statistical model of interest here has been described in detail in previous publications,[17,21] and needs only to be summarized briefly in order to fix notation.

We start by assuming that our system can be described by a single scalar order parameter $c(\vec{r})$, which we can visualize as the average concentration of one of the components of a binary solution in some region around the position $\vec{r}$. [Alternatively, $c(\vec{r})$ might be the local magnetization of an Ising ferromagnet.] In terms of $c(\vec{r})$, we write a coarse-grained Helmholtz free energy in the Ginzburg-Landau form:

$$F\{c\} = \int dr\,[\tfrac{1}{2}K(\nabla c)^2 + f(c)]. \tag{2.1}$$

The meaning of the coarse-graining procedure has been discussed in Ref. 21. What will be crucial for the following analysis is that we shall take the coarse-graining volume to be proportional to the cube of the equilibrium correlation length ξ. That is, at any given temperature, we shall assume that $c(\vec{r})$ is a smooth function on the scale of ξ, and that $F\{c\}$ has been computed by evaluating a partition sum over all fluctuations with wavelengths shorter than ξ. This procedure permits us to use $c(\vec{r})$ to describe relatively large-scale phase separation and coarsening, while still assuming that F, although nonconvex, is simply related to the true equilibrium properties of the system. The significance of this choice of coarse-graining size will become clearer when we come to choosing system parameters in Sec. IV.

To describe the kinetics of this system, we start with a continuity equation of the form

$$\frac{\partial c}{\partial t} = -\vec{\nabla}\cdot\vec{j}, \tag{2.2}$$

where $\vec{j}$ is a current density which describes the interdiffusion of atomic species and is given by

$$\vec{j}(\vec{r}) = -M\vec{\nabla}\frac{\delta F}{\delta c(\vec{r})} = -M\vec{\nabla}\left(-K\nabla^2 c + \frac{\partial f}{\partial c}\right). \tag{2.3}$$

Here, M is a phenomenological quantity which is proportional to a mobility and which we shall take to be a constant, independent of $c(\vec{r})$. (But see the discussion of M in Sec. V.) In order to construct a statistical theory based on the equations of motion (2.2) and (2.3), we formally add a Langevin force to the right-hand side of (2.2). The latter force describes the random part of the interaction between the composition variations and the heat bath. We then can derive a master equation for the distribution-functional $\rho\{c\}$ defined on the space of functions $c(\vec{r})$. This master equation has

the form of a functional continuity equation:

$$\frac{\partial \rho\{c\}}{\partial t} = -\int d\vec{r}\,\frac{\delta J(\vec{r})}{\delta c(\vec{r})}, \tag{2.4}$$

where the probability current $J(\vec{r})$ is given by

$$J(\vec{r}) = M\nabla^2\left(\frac{\delta F}{\delta c(\vec{r})}\rho + k_B T\frac{\delta \rho}{\delta c(\vec{r})}\right). \tag{2.5}$$

Together with the specification of the coarse-graining length (which plays the role of a cutoff), Eqs. (2.4) and (2.5) constitute a mathematically complete statement of the model upon which all of our subsequent analysis will be based.

As in our previous work, we shall focus attention primarily on a calculation of the structure factor $\hat{S}(k)$, which is the Fourier transform of the two-point correlation function $S(r)$. $\hat{S}(k)$ is directly proportional to the x-ray scattering intensity at wave-vector transfer $\vec{k}$. Let c_0 denote the average composition of the system, and define the fluctuation variable $u(\vec{r}, t)$ to be

$$u(\vec{r}, t) = c(\vec{r}, t) - c_0. \tag{2.6}$$

Then

$$S(|\vec{r} - \vec{r}_0|, t) \equiv \langle u(\vec{r}, t)u(\vec{r}_0, t)\rangle \tag{2.7}$$

and

$$\hat{S}(k, t) \equiv \int d\vec{r}\,S(r, t)e^{i\vec{k}\cdot\vec{r}}. \tag{2.8}$$

Here, the angular brackets denote averages with respect to the distribution functional ρ, and we have assumed translational symmetry after averaging.

The equation of motion for S is obtained by multiplying the master equation by $u(\vec{r})u(\vec{r}_0)$ and integrating over the space of functions u. The resulting equation is best written in the Fourier representation, where it takes the form

$$\frac{\partial \hat{S}(k)}{\partial t} = -2Mk^2\left[\left(Kk^2 + \frac{\partial^2 f}{\partial c_0^2}\right)\hat{S}(k) + \frac{1}{2}\frac{\partial^3 f}{\partial c_0^3}\hat{S}_3(k) + \frac{1}{6}\frac{\partial^4 f}{\partial c_0^4}\hat{S}_4(k) + \cdots\right] + 2Mk_B T k^2. \tag{2.9}$$

The quantities that we have denoted $\hat{S}_n$ are the Fourier transforms of the higher-order two-point correlation functions:

$$S_n(|\vec{r} - \vec{r}_0|) \equiv \langle u^{n-1}(\vec{r})u(\vec{r}_0)\rangle. \tag{2.10}$$

(We omit the subscript on S for the case $n = 2$.) Equation (2.9) is the first of a hierarchy of increasingly complex equations of motion for high-order multipoint correlation functions which one may obtain by taking higher moments of the master equation. Our problem is to devise a physically plausible and mathematically tractable scheme for truncating this hierarchy.

Before turning to the new computational scheme to be introduced here, it will be useful to review two simpler approximations which have been studied previously. First, if we neglect all of the higher-order terms in (2.9), we obtain Cook's[15] linear equation of motion for $\hat{S}$:

$$\frac{\partial \hat{S}(k)}{\partial t} = 2R(k)\hat{S}(k) + 2Mk_B T k^2, \tag{2.11}$$

where the amplification factor, $R(k)$, is given by

$$R(k) = -Mk^2\left(Kk^2 + \frac{\partial^2 f}{\partial c_0^2}\right). \tag{2.12}$$

For negative values of $\partial^2 f/\partial c_0^2$, that is, for values of c_0 within the classical spinodal region, $R(k)$ will be positive for $k < k_c$, where

$$k_c = \left(\frac{1}{k}\left|\frac{\partial^2 f}{\partial c_0^2}\right|\right)^{1/2}, \tag{2.13}$$

and will have a maximum at $k = k_m = k_c/\sqrt{2}$. Fluctuation modes with k near k_m, in this approximation, are expected to grow exponentially in time, resulting in a precipitation pattern with near-periodicity at wavelength $\lambda_m = 2\pi/k_m$. The standard metallurgical analysis of x-ray data, as described in Ref. 2 for example, has been to identify $R(k)$ as the logarithmic time derivative of the scattering intensity, and to plot $R(k)/k^2$ versus k^2 with the expectation of finding a straight line for spinodal systems. For reasons which will become apparent, the resulting plot often turns out to be strongly nonlinear.[7]

The "mean-field" approximation[19] can be obtained from (2.9) by assuming that $\rho\{c\}$ is always a Gaussian distribution on the function $u(\vec{r})$, centered at $u = 0$. Then all odd correlation functions vanish, and

$$\hat{S}_4(k) \cong 3\langle u^2\rangle\hat{S}(k), \tag{2.14}$$

with

$$\langle u^2\rangle = \frac{1}{(2\pi)^3}\int d\vec{k}\,\hat{S}(k). \tag{2.15}$$

The resulting equation of motion for $\hat{S}$ has the same form as in the linear theory, but the previously constant quantity $\partial^2 f/\partial c_0^2$ is now replaced by the time-dependent expression

$$\frac{\partial^2 f}{\partial c_0^2} + \frac{1}{2}\frac{\partial^4 f}{\partial c_0^4}\langle u^2(t)\rangle.$$

[We have dropped higher terms in the expansion of $f(c)$.] Because $\langle u^2\rangle$ is a positive, increasing function of time, the characteristic wave number k_c must decrease. That is, the mean-square fluctuations, via the nonlinear part of $\partial f/\partial c$, cause

a qualitatively correct coarsening of the precipitation pattern. But there are obviously serious defects in this scheme. The fluctuations $u(\vec{r})$ cannot be expected to remain small for any appreciable time during the decomposition. On the contrary, one expects the distribution on u eventually to become peaked near those values of u such that c_0+u is equal to one or the other of the equilibrium concentrations. An equally serious defect of this approximation is its neglect of the third-order term in (2.9). Near the classical spinodal, the quantity $\partial^2 f/\partial c_0^2$ is small, and it is the third-order term, proportional to $\partial^3 f/\partial c_0^3$, which characterizes the instability. As has been emphasized by Cahn,[16] the resulting decomposition occurs via fluctuations in u which are not at all symmetric about $u=0$ (rather like the motion of a particle in a cubic potential). Because it is unable to take account of these asymmetric fluctuations, the mean-field approximation gives a poor picture of phase separation near the boundaries of the spinodal region. The approximation scheme to be introduced in the following section has been developed specifically for the purpose of overcoming the above limitations of the mean-field method.

III. GENERAL SCHEME OF APPROXIMATIONS

Returning to Eqs. (2.9) and (2.10), we note that each of the higher-order correlation functions that we need involves only two spatial positions, $\vec{r}$ and $\vec{r}_0$. Thus, a knowledge of the two-point distribution function, $\rho_2[u(\vec{r}),u(\vec{r}_0)]$, would be sufficient to determine the right-hand side of (2.9). By ρ_2, we mean the normalized distribution function obtained from the full functional $\rho\{u\}$ by integrating over u space while holding the values of u fixed at points $\vec{r}$ and $\vec{r}_0$. Of course, an attempt to write exact equations of motion for ρ_2 would lead to a hierarchy of ρ_n equations even less tractable than the correlation-function hierarchy with which we started. What we shall do instead is guess a reasonable form for ρ_2 which we can compute in terms of known functions.

The ansatz for ρ_2 that we have found most useful is the following. Let $\rho_1(u)$ be the single-point distribution function, and write

$$\rho_2[u(\vec{r}),u(\vec{r}_0)]\cong\rho_1[u(\vec{r})]\rho_1[u(\vec{r}_0)] \times\{1+\gamma(|\vec{r}-\vec{r}_0|)u(\vec{r})u(\vec{r}_0)\}. \tag{3.1}$$

One may think of the quantity in curly brackets as the first two terms in a power series expansion in the two variables $u(\vec{r})$ and $u(\vec{r}_0)$. Cutting off this expansion after the first nontrivial term, however, turns out to produce very important simplifications in the subsequent analysis.

The function $\rho_1(u)$ must be normalized in such a way that

$$\int_{-\infty}^{\infty}\rho_1(u)\,du=1 \tag{3.2}$$

and

$$\int_{-\infty}^{\infty}\rho_1(u)u\,du=0. \tag{3.3}$$

The second of these conditions follows from the definition of the variable u in Eq. (2.6). From Eqs. (3.2) and (3.3), it follows that ρ_2 is automatically normalized:

$$\int_{-\infty}^{\infty}\int_{-\infty}^{\infty}\rho_2(u,u_0)\,du\,du_0=1, \tag{3.4}$$

and that

$$\rho_1(u)=\int_{-\infty}^{\infty}\rho_2(u,u_0)\,du_0. \tag{3.5}$$

The correlation function is

$$S(r)=\langle u^2\rangle^2\gamma(r). \tag{3.6}$$

Using (3.6) to identify the function $\gamma(r)$ in (3.1), we now can write:

$$S_n(r)\cong\frac{\langle u^n\rangle}{\langle u^2\rangle}S(r). \tag{3.7}$$

Therefore, within the approximation suggested here, the higher-order correlation functions of the form (2.10) all have the same r dependence as S. This is not unreasonable, especially for the long-range correlations that are of interest. The resulting form of Eq. (2.9) is

$$\frac{\partial\hat{S}(k)}{\partial t}=-2Mk^2(Kk^2+A)\hat{S}(k)+2Mk_BTk^2, \tag{3.8}$$

where

$$A=\sum_{n=2}^{\infty}\frac{1}{(n-1)!}\frac{\partial^n f}{\partial c_0^n}\frac{\langle u^n\rangle}{\langle u^2\rangle} =\frac{1}{\langle u^2\rangle}\left\langle u\frac{\partial f(c_0+u)}{\partial u}\right\rangle. \tag{3.9}$$

Note that the k dependence of this equation has become mathematically trivial, and the only two-point function which appears explicitly is S itself.

There remains only the evaluation of the time-dependent quantity $A(t)$ in order to complete the approximation scheme. $A(t)$ is a one-point function which is easily evaluated once ρ_1 is known. In fact, ρ_1 is completely determined by the ansatz (3.1). The equation of motion for ρ_1, obtained by integrating the master equation over u space while holding u fixed at just one position $\vec{r}$, involves only the distribution functions ρ_1 and ρ_2. But ρ_2 is given by (3.1); thus, the hierarchy of ρ_n equations is

closed at $n=1$.

To derive the equation which determines ρ_1, it is necessary to use a formalism that takes explicit account of the smoothness of $u(\vec{r})$ implied by the coarse-graining assumption. A simple way to do this is to replace the continuous position variable $\vec{r}$ by a denumerable set of sites r_α on a lattice whose spacing is the coarse-graining length a. The function $u(\vec{r})$ is then replaced by a set of variables u_α. The point here is that quantities of the form $\langle u(r)^n\rangle$ have meaning only in terms of the coarse-graining assumption. For example, if u were to represent an average of Ising spins whose values are ±1, then $\langle u^2\rangle$ would be unity for the special case of a coarse-graining length equal to just one microscopic lattice spacing, but would be some smaller, temperature- and time-dependent quantity otherwise. Another way of seeing this is to note that $\langle u^2\rangle$, as given by the Fourier integral in (2.15) for example, is strongly cutoff dependent.

In the coarse-grained cellular notation suggested above, the master equation has the form

$$\frac{\partial\rho\{u\}}{\partial t}=-\sum_\alpha\frac{\partial J_\alpha\{u\}}{\partial u_\alpha}, \tag{3.10}$$

where

$$J_\alpha=J(r_\alpha)=\frac{M}{a^3}\sum_\beta\Delta_{\alpha\beta}\left(\frac{\partial F}{\partial u_\beta}\rho+k_BT\frac{\partial\rho}{\partial u_\beta}\right), \tag{3.11}$$

and

$$\frac{\partial F}{\partial u_\beta}=-Ka^3\sum_{\beta'}\Delta_{\beta\beta'}u_{\beta'}+a^3\frac{\partial f(u_\beta)}{\partial u_\beta} \tag{3.12}$$

is the finite-difference representation of the quantity $a^3\delta F/\delta u(\vec{r})$. The matrix $\Delta_{\alpha\beta}$ represents the operator ∇^2 appearing in Eq. (2.5). Integrating over all but one of the u_α, we obtain

$$\begin{aligned}\frac{\partial\rho_1(u_\alpha)}{\partial t}&=-\frac{\partial}{\partial u_\alpha}\left(\prod_{\beta\neq\alpha}\int_{-\infty}^{\infty}du_\beta\right)J_\alpha\{u\}\\&=-M\frac{\partial}{\partial u_\alpha}\sum_\gamma\Delta_{\alpha\gamma}\left[\left(-K\Delta_{\gamma\alpha}u_\alpha+\delta_{\gamma\alpha}\frac{\partial f(u_\alpha)}{\partial u_\alpha}\right)\rho_1(u_\alpha)-\sum_{\beta\neq\alpha}\int_{-\infty}^{\infty}du_\beta\left(-K\Delta_{\gamma\beta}u_\beta+\delta_{\gamma\beta}\frac{\partial f(u_\beta)}{\partial u_\beta}\right)\rho_2(u_\alpha,u_\beta)\right]\\&\quad-\frac{Mk_BT\Delta_{\alpha\alpha}}{a^3}\frac{\partial^2\rho_1}{\partial u_\alpha^2}.\end{aligned} \tag{3.13}$$

As mentioned above, we now may use (3.1) to eliminate ρ_2 in this equation. The result is an equation of the form

$$\frac{\partial\rho_1}{\partial t}=M\frac{\partial}{\partial u}\left(G(u)\rho_1+k_BT\frac{\Delta}{a^3}\frac{\partial\rho_1}{\partial u}\right), \tag{3.14}$$

where Δ denotes the α-independent constant $|\Delta_{\alpha\alpha}|$,

$$G(u)=W\frac{u}{\langle u^2\rangle}+\Delta\left(\frac{\partial f}{\partial u}-\left\langle\frac{\partial f}{\partial u}\right\rangle-\frac{u}{\langle u^2\rangle}\left\langle u\frac{\partial f}{\partial u}\right\rangle\right), \tag{3.15}$$

and

$$W=-\sum_{\gamma,\beta}\Delta_{\alpha\beta}(-K\Delta_{\beta\gamma}+A\delta_{\beta\gamma})S_{\gamma\alpha}. \tag{3.16}$$

In (3.15), as in (3.9), f is always to be evaluated at c_0+u. Finally, we can eliminate the fictitious lattice sums by returning to a Fourier representation. Let $k_{\max}$ be the radius of the Wigner-Seitz sphere in Fourier space corresponding to the coarse-graining length a:

$$k_{\max}^3=6\pi^2/a^3. \tag{3.17}$$

Then

$$\Delta=\frac{a^3}{2\pi^2}\int_0^{k_{\max}}k^4\,dk=\tfrac{3}{5}k_{\max}^2 \tag{3.18}$$

and

$$W=\frac{1}{2\pi^2}\int_0^{k_{\max}}k^4(Kk^2+A)\hat{S}(k)\,dk. \tag{3.19}$$

Together, Eqs. (3.8) and (3.14) constitute a closed mathematical system which can be solved numerically by straightforward computational methods. Equation (3.14), however, has the form of a diffusion equation for a particle whose position is u and which is subject to a time-dependent force, $-G(u)$. Available numerical techniques for solving such an equation are time consuming and subject to unpredictable instabilities. In order to avoid this difficulty, we have resorted to an approximation which we have used for a similar equation in Ref. 18. The idea is to assume a simple, parametrized, functional form for $\rho_1(u)$, and then to derive and solve a small set of ordinary differential equations for these parameters instead of solving the full partial differential equation (3.14).

The form we choose for ρ_1 is a sum of displaced Gaussians:

$$\rho_1(u)=\frac{a_1}{\sigma(2\pi)^{1/2}}\exp\left(-\frac{(u-b_1)^2}{2\sigma^2}\right)+\frac{a_2}{\sigma(2\pi)^{1/2}}\exp\left(-\frac{(u+b_2)^2}{2\sigma^2}\right). \tag{3.20}$$

The normalization conditions (3.2) and (3.3) require that

$$a_1 = b_2/(b_1+b_2), \quad a_2 = b_1/(b_1+b_2). \tag{3.21}$$

Thus, there remain three time-dependent parameters, σ, b_1, and b_2 to be determined. These parameters have been chosen to convey some qualitative information about the state of the system. For an undecomposed system, b_1 and b_2 will be small compared to σ, indicating a fluctuation distribution with a single peak at $u=0$. As the spinodal reaction nears completion, on the other hand, we expect to see a well-defined, doubly peaked distribution for which σ is appreciably smaller than the separation between the peaks, i.e., $\sigma \ll b_1+b_2$. Note also that the ansatz for ρ_1 is set up to deal with asymmetric situations in which $b_1 \neq b_2$.

The calculation of the above three parameters can be based on the solution of three moment equations derived from (3.14). That is, we multiply (3.14) by u^2, u^3, and u^4, and then integrate over u to obtain equations for $\langle u^2\rangle$, $\langle u^3\rangle$, and $\langle u^4\rangle$. In this way, we find

$$\frac{d}{dt}\langle u^2\rangle = 2M[-W + k_B T(\Delta/a^3)] \tag{3.22}$$

$$\frac{d}{dt}\langle u^3\rangle = -3M\left[W\frac{\langle u^3\rangle}{\langle u^2\rangle} + \Delta\sum_{n=3}^{\infty}\frac{1}{(n-1)!}\frac{\partial^n f}{\partial c_0^n} \times\left(\langle u^{n+1}\rangle - \langle u^2\rangle\langle u^{n-1}\rangle - \frac{\langle u^3\rangle\langle u^n\rangle}{\langle u^2\rangle}\right)\right]. \tag{3.23}$$

For numerical accuracy at early times, when the fluctuations are still small, it is better to compute

$$\langle u^4\rangle_c \equiv \langle u^4\rangle - 3\langle u^2\rangle^2 \tag{3.24}$$

rather than to compute $\langle u^4\rangle$ directly. The relevant equation is

$$\frac{d}{dt}\langle u^4\rangle_c = 4M\left[-W\frac{\langle u^4\rangle_c}{\langle u^2\rangle} + \Delta\sum_{n=3}^{\infty}\frac{1}{(n-1)!}\frac{\partial^n f}{\partial c_0^n} \times\left(\langle u^{n+2}\rangle - \langle u^3\rangle\langle u^{n-1}\rangle - \frac{\langle u^4\rangle\langle u^n\rangle}{\langle u^2\rangle}\right)\right]. \tag{3.25}$$

The next step is to express the right-hand sides of Eqs. (3.22), (3.23), and (3.25) in terms of the three basic parameters of Eq. (3.20). We have

$$\langle u^2\rangle = \sigma^2 + b_1 b_2, \tag{3.26}$$

$$\langle u^3\rangle = b_1 b_2 (b_1 - b_2), \tag{3.27}$$

$$\langle u^4\rangle_c = b_1 b_2[(b_1-b_2)^2 - 2b_1 b_2]. \tag{3.28}$$

Any higher moments which appear in (3.23) and (3.25) can also be expressed in terms of b_1, b_2, and σ via Eq. (3.20). For example, if we cut off the expansion of f after the fourth term, as we shall do for the specific calculations to be described in Secs. V and VI, then we shall need $\langle u^5\rangle$ and $\langle u^6\rangle$, which are given by

$$\langle u^5\rangle = b_1 b_2 (b_1 - b_2)(10\sigma^2 + b_1^2 + b_2^2), \tag{3.29}$$

$$\langle u^6\rangle = 15\sigma^6 + 45\sigma^4 b_1 b_2 + 15\sigma^2 b_1 b_2 (b_1^2 - b_1 b_2 + b_2^2) + b_1 b_2 (b_1^4 - b_1^3 b_2 + b_1^2 b_2^2 - b_1 b_2^3 + b_2^4). \tag{3.30}$$

Our numerical procedure is as follows. Given values of b_1, b_2, and σ at a time t, we compute new values of $\langle u^2\rangle$, $\langle u^3\rangle$, $\langle u^4\rangle_c$ at time $t+\Delta t$ using Eqs. (3.22)–(3.25) along with (3.29) and (3.30). We also compute new values of $\hat{S}(k)$ from Eq. (3.8). Then we invert Eqs. (3.26)–(3.28) to obtain new values of b_1, b_2, and σ. This inversion is performed by noticing that the quantity $b_1 b_2$ satisfies the cubic equation:

$$(b_1 b_2)^3 + \tfrac{1}{2}(b_1 b_2)\langle u^4\rangle_c - \tfrac{1}{2}\langle u^3\rangle^2 = 0, \tag{3.31}$$

which is solved by successive approximations. Given $(b_1 b_2)$, we easily obtain each of the three parameters separately from (3.26) and (3.27). Finally, we recompute A from (3.9) and W from (3.19), thus completing the iteration cycle.

IV. SCALING ANALYSIS

Before starting a numerical study of the approximation scheme outlined in the preceding section, it is necessary to reduce the equations to dimensionless forms in order to find out how various physical parameters enter into the theory. We shall see that, if one is close enough to a critical point that simple scaling laws become valid, only one model-dependent parameter is needed to describe the decomposition process at all temperatures. Away from the critical point, this parameter will become weakly temperature dependent, but the scaled form of the theory will continue to be useful.

To begin this analysis, we shall have to assume that the free energy $f(c)$, apart from linear terms in c, is symmetric about some value of composition, say, $c_{\rm sym}$. We can then work with the variable $X \equiv c - c_{\rm sym}$. The coexistence curve, or miscibility gap, is[22]

$$X_s(T) \approx \pm B\epsilon^{\beta}, \quad \epsilon = 1 - T/T_c. \tag{4.1}$$

The appropriate scaling form for $f(X)$ is

$$f(X) = (k_B T/a^3) f_0 \phi(X/X_s), \tag{4.2}$$

where a is the coarse-graining length defined previously, ϕ is a dimensionless function, and f_0 is a constant defined by the normalization of ϕ, chosen here to be

$$\phi(0) = \phi'(0) = 0, \quad \phi''(0) = -1. \tag{4.3}$$

If f is the coarse-grained free energy computed as described at the beginning of Sec. II, then we must have

$$\phi'(\pm 1)=0; \tag{4.4}$$

that is, $f(X)$ must have its minima at $X=\pm X_s$.

To evaluate, f_0, we examine the differential susceptibility

$$\chi_s=(1/a_0^3)\hat{S}(k=0)\approx C\epsilon^{-\gamma}, \tag{4.5}$$

where a_0 is the underlying lattice spacing, and C is a constant defined by Fisher.[22] The coarse-graining assumption requires that f contain all of the thermodynamically important fluctuations, i.e., those with wavelengths up to the correlation length ξ; thus, a simple, mean-field approximation ought to be adequate for $\hat{S}(0)$:

$$\hat{S}(0)\cong k_BT\Big/\left(\frac{\partial^2 f}{\partial X^2}\right)\Big|_{X=X_s}=\frac{a^3X_s^2}{f_0\phi''(1)}. \tag{4.6}$$

Combining (4.1), (4.5), and (4.6), we find

$$f_0=\left(\frac{a}{a_0}\right)^3\frac{X_s^2}{\chi_s\phi''(1)}\approx\left(\frac{a}{a_0}\right)^3\frac{B^2}{C\phi''(1)}. \tag{4.7}$$

Finally, and most important, if we choose a such that the cutoff $k_{\max}$ in (3.17) is proportional to the inverse correlation length, say, $k_{\max}=\alpha/\xi$ where α is a constant of order unity, then

$$a=[(6\pi^2)^{1/3}/\alpha]\,\xi, \tag{4.8}$$

and

$$f_0\approx\frac{6\pi^2}{\alpha^3}\left(\frac{\xi_0}{a_0}\right)^3\frac{B^2}{C\phi''(1)} \tag{4.9}$$

is independent of ϵ. Here we have used

$$\xi\approx\xi_0\epsilon^{-\nu'} \tag{4.10}$$

along with the scaling relation $2\beta+\gamma'=3\nu'$. Note that if we choose the standard Ginzburg-Landau polynomial for ϕ (quadratic plus quartic), then Eqs. (4.3) and (4.4) require $\phi''(1)=2$.

Within the same mean-field approximation used in (4.6), we have

$$\frac{k_{\max}^2}{\alpha^2}=\frac{1}{\xi^2}\cong\frac{1}{K}\frac{\partial^2 f}{\partial X_s^2}=\frac{k_BTf_0}{Ka^3X_s^2}\phi''(1). \tag{4.11}$$

It will turn out to be useful to define a wave number k_c such that

$$k_c^2=\frac{k_{\max}^2}{\alpha^2\phi''(1)}=\frac{k_BTf_0}{Ka^3X_s^2}\approx\frac{\epsilon^{2\nu'}}{\phi''(1)\xi_0^2}. \tag{4.12}$$

This k_c may be identified as the largest wave number for which the linear approximation (2.11) predicts an instability when $X_0=c_0-c_{\rm sym}=0$. We shall use k_c^{-1} as a natural unit of length, and shall define the reduced wave number q by

$$k=qk_c. \tag{4.13}$$

We now make the following scaling transformations. We introduce a dimensionless time variable τ:

$$\tau=\frac{2Mk_BTk_c^2f_0}{a^3X_s^2}t\approx\frac{2Mk_BT\epsilon^{\gamma'+2\nu'}}{a_0^3\xi_0^2C\phi''(1)^2}t; \tag{4.14}$$

and a dimensionless structure factor $\mathcal{S}$:

$$\mathcal{S}(q,\tau)=\frac{f_0}{a^3X_s^2}\hat{S}(k,t)\approx\frac{\epsilon^{\gamma'}}{Ca_0^3\phi''(1)}\hat{S}(k,t). \tag{4.15}$$

Then Eq. (3.8) reduces to the form

$$\frac{\partial\mathcal{S}}{\partial\tau}=-q^2(q^2-\mu)\mathcal{S}+q^2, \tag{4.16}$$

where

$$\mu\equiv-\frac{1}{\langle y^2\rangle}\left\langle y\frac{\partial\phi(x_0+y)}{\partial y}\right\rangle \tag{4.17}$$

and

$$y=u/X_s,\quad x_0=X_0/X_s. \tag{4.18}$$

Equation (3.14) transforms into an equation of motion for the distribution over the reduced fluctuation variable y. After some algebra, we find

$$\frac{\partial\rho_1}{\partial\tau}=\frac{3\alpha^2\phi''(1)}{10f_0}\frac{\partial}{\partial y}\left(g(y)\rho_1+\frac{\partial\rho_1}{\partial y}\right), \tag{4.19}$$

where

$$g(y)=\frac{5\bar{\mathcal{S}}}{\alpha^5[\phi''(1)]^{5/2}}\frac{y}{\langle y^2\rangle}+f_0\left(\frac{\partial\phi}{\partial y}-\left\langle\frac{\partial\phi}{\partial y}\right\rangle-\frac{y}{\langle y^2\rangle}\left\langle y\frac{\partial\phi}{\partial y}\right\rangle\right) \tag{4.20}$$

and

$$\bar{\mathcal{S}}\equiv\int_0^{\alpha[\phi''(1)]^{1/2}}q^2(q^2-\mu)\mathcal{S}(q)\,dq. \tag{4.21}$$

In analogy with (3.15), ϕ in (4.20) denotes $\phi(x_0+y)$. Given a functional form for ϕ, the only input parameters which are needed in Eqs. (4.16) and (4.19) are x_0 and f_0. It is f_0 which is the only nontrivial system-dependent parameter remaining in the scaled form of the theory.

V. KINETIC ISING MODEL

Throughout the rest of this paper, we shall couch our numerical results in terms of the kinetic Ising model as used by Bortz *et al.*[10] We shall see immediately that, because of certain further approximations that we have made, our calculations are not yet realistic enough to permit reliable quantitative comparisons with three-dimensional Monte Carlo data.[23] Nevertheless, the Ising model does provide us with a useful conceptual basis for discussion, and our information about it is com-

plete enough that semiquantitative comparisons will be meaningful.

Perhaps the most serious assumption that we shall make is that ϕ has the Ginzburg-Landau form:

$$\phi(x) = -\tfrac{1}{2}x^2 + \tfrac{1}{4}x^4, \quad x = X/X_s. \tag{5.1}$$

In the scaling region near the critical point, however, ϕ must be identified as the fixed-point Hamiltonian which has been defined and computed by Wilson,[24] and for which a sixth-order term is known to be important. Our neglect of this term means that we are going to overestimate the magnitude of the fluctuations during the later stages of the decomposition, and that even our early-stage results will be quantitatively incorrect for values of X_0 near the spinodal.

A second limitation comes from our use of the conventional power-law approximations for the ϵ dependence of the quantities ξ, X_s, and χ_s. This will limit the accurate applicability of our results to values of ϵ not much larger than 10^{-2}. Because of critical slowing down [note the factor $\epsilon^{\gamma'+2\nu'}$ in (4.14)], Monte Carlo experiments take a very long time and are essentially impossible in this region. On the other hand, accurate calculations at larger ϵ's will require separate evaluations of all of the relevant parameters [as well as $\phi(x)$] at each temperature. To achieve some degree of generality, therefore, we shall simply use available data from the scaling region.

The specific data that we shall use are the following numerical estimates for the simple-cubic Ising model[22,25]:

$$\begin{aligned} &B = 1.57, \quad \beta = 0.339 \text{ (assuming scaling)}, \\ &C = 0.193, \quad \gamma' = \tfrac{5}{4}, \\ &\xi_0/a_0 = 0.248, \quad \nu' = \tfrac{9}{14}. \end{aligned} \tag{5.2}$$

The quantities B, C, and ξ_0 are defined in Eqs. (4.1), (4.5), and (4.10) respectively. Given these quantities, and using $\phi''(1) = 2$ and $\alpha = 1$, we have

$$f_0 \cong 5.77. \tag{5.3}$$

We also have

$$k_c \cong 2.85\epsilon^{9/14}/a_0 \tag{5.4}$$

and

$$\hat{S}(k) = 0.386 a_0^3 \epsilon^{-5/4} S(q). \tag{5.5}$$

In order to evaluate the ratio τ/t from Eq. (4.14), we must first make some estimate of the rate factor M. This problem has been studied by Kawasaki,[26] who has obtained the same scaling law for spin diffusion that we have found in (4.14). To make a simple estimate of the magnitude of M, we assume that M is a purely kinematical quantity, i.e., that it depends on the frequency of attempted exchanges and on geometrical properties of the system, but not on any dynamical quantities such as interaction energies. Thus, we can evaluate M by looking at the purely noninteracting spin-diffusion problem.

Let $X_i(t)$ denote the average spin at a site i on a simple cubic lattice at time t. Suppose that there are no interactions between these spins, but that a spin-conserving stochastic process is defined, in accord with Bortz *et al.*,[10,23] as follows. A site is chosen at random; then a nearest neighbor to this site is chosen, also at random. If the spins on these sites have opposite signs, then these spins are exchanged with probability $\frac{1}{2}$. This process is considered to be a single "trial," and time t is measured in "trials" per lattice site. The resulting motion of the average spin $X(\vec{r}, t)$ is described by a diffusion equation of the form

$$\frac{\partial X}{\partial t} = \frac{a_0^2}{12}\nabla^2 X, \tag{5.6}$$

where a_0 is the lattice spacing. To make contact with the definition of M in Eq. (2.3), we must equate the diffusion constants:

$$\frac{a_0^2}{12} \cong M\left(\frac{\partial^2 f}{\partial X^2}\right)_{\text{noninteracting}}. \tag{5.7}$$

For the free energy in (5.7), we need only the entropy of a system of noninteracting Ising spins (± 1) with magnetization S; that is,

$$\frac{\partial^2 f}{\partial X^2} = \frac{k_B T}{a_0^3}\frac{1}{1 - X^2}. \tag{5.8}$$

Thus,

$$M \cong (a_0^5/12 k_B T)(1 - X^2). \tag{5.9}$$

Note that, in contradiction to our original assumption, M does turn out to have a composition dependence. This X dependence of M might be quite important for late-stage spinodal decomposition at low temperatures, where the values of X will fluctuate between ± 1. For present purposes, however, we shall simply set $X = X_0$ in (5.9). Finally, returning to (4.14), we have

$$\begin{aligned} \frac{\tau}{t} &\approx \frac{1}{24}\left(\frac{a_0}{\xi_0}\right)^2 \frac{(1 - X_0^2)}{C}\epsilon^{\gamma'+2\nu'} \\ &\cong 3.51(1 - X_0^2)\epsilon^{2.536}. \end{aligned} \tag{5.10}$$

The last quantity that we must compute in order to complete the connection between our theory and kinetic Ising results is the initial value of the reduced structure factor, $S(q, \tau = 0)$. The standard Monte Carlo experiment[9,10,23] simulates a rapid quench from high temperature into the two-phase region. That is, one starts at $t = 0$ with a completely uncorrelated array of Ising spins. In a coarse-

graining cell containing $(a/a_0)^3$ lattice sites, the mean-square order parameter will be $\langle X^2\rangle = (a_0/a)^3$. Thus, from Eqs. (2.7) and (2.8),

$$\hat{S}(k, t=0) = a^3\langle X^2\rangle = a_0^3, \tag{5.11}$$

and, from Eq. (4.15),

$$\mathcal{S}(q, t=0) = 1/\chi_s\phi''(1) \cong 2.59\epsilon^{5/4}. \tag{5.12}$$

This result has the unfortunate effect of destroying the temperature independence of our scaled theory. In all of the calculations described in Sec. VI, we have started with $\mathcal{S}(q, t=0)=0$. This choice of initial condition is going to have an effect on our calculations only for very small reduced times τ or for large values of ϵ.

VI. RESULTS AND INTERPRETATION

The computational scheme described in the previous three sections has been carried out numerically, and selected results are shown in the accompanying figures. We have used the simplest possible finite-difference method for integration of all of the differential equations. In order not to have our τ intervals limited by the short relaxation times implied by the $\mathcal{S}$ equation (4.16), for large q, we have built into the program a check to see where $\mathcal{S}$ is well approximated by $(q^2-\mu)^{-1}$, and have inserted that formula for increasingly large pieces of the high-q tail at later times τ. In this way the τ intervals can be increased gradually throughout the computation and stability can be maintained.

In Fig. 1, we show $\mathcal{S}(q)$ curves for selected times τ for $x_0=0$. Note that the peak in $\mathcal{S}$ moves toward smaller q as τ increases. There is no hint of exponential behavior of $\mathcal{S}$ for any value of q. The linear theory does predict fairly accurately

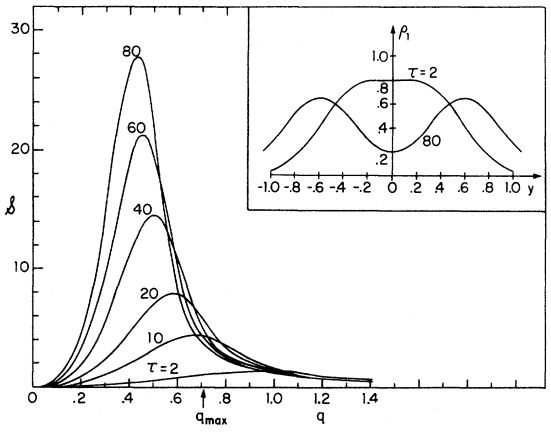

FIG. 1. Structure factor $\mathcal{S}(q)$ for $f_0=5.8$, $x_0=0$ computed at various times τ. The inset depicts the distribution function $\rho_1(y)$ at two of these times.

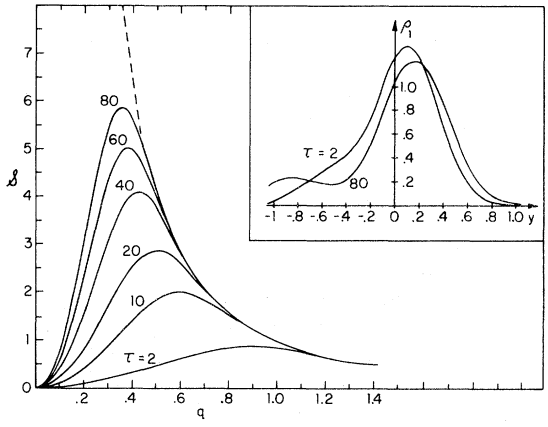

FIG. 2. Same as Fig. 1 but for $x_0=1/\sqrt{3}$. The dashed line indicates the envelope $1/q^2$.

the position of the peak at very early times ($\tau \cong 10$). This position, $q_{max}=1/\sqrt{2}$ is indicated below the graph. In the inset in Fig. 1 we show the functions $\rho_1(y)$ corresponding to two of the $\mathcal{S}(q)$ curves on the left. As expected, ρ_1 is initially peaked at $y=0$, but this peak splits symmetrically and eventually develops into two distinct peaks which are slowly separating from one another.

Figure 2 is drawn in analogy to Fig. 1, but this time for $x_0=1/\sqrt{3}$. This value of x_0 places us exactly at the classical spinodal where $\partial^2 f/\partial x_0^2$ vanishes. Thus, the linear theory would predict $q_{max}=0$ and no decomposition at all. Instead, we see that a broad but well-defined peak does develop, albeit with considerably less intensity than for $x_0=0$. This peak shifts to the left with increasing τ, but the cross-over phenomenon, that is, the leftward shift of the large-q tail of $\mathcal{S}$, does not occur. The inset in Fig. 2 shows two corresponding ρ_1 curves. There is, of course, an asymmetry here, reflecting the fact that the fluctuations are developing in accord with the lever rule. More interesting is the fact that two distinct peaks have appeared by the time $\tau=80$, indicating that a true phase separation is taking place.

Some further insight into what is happening here can be obtained by examining the function $\mu(\tau)$, defined in Eq. (4.17). For the specific function ϕ that we have chosen in Eq. (5.1), we have

$$\mu = 1 - 3x_0^2 - 3x_0\langle y^3\rangle/\langle y^2\rangle - \langle y^4\rangle/\langle y^2\rangle. \tag{6.1}$$

Note that, in Eq. (4.16), it is μ which determines the instantaneous stability of the Fourier modes whose intensities are represented by $\mathcal{S}(q)$. Modes with $q^2<\mu$ will be growing unstably. Those with $q^2>\mu$ may also be growing; but these modes are relaxing toward $(q^2-\mu)^{-1}$, which may, of course, be quite large. This verbal picture is complicated by the fact that μ itself is a function of τ, as shown

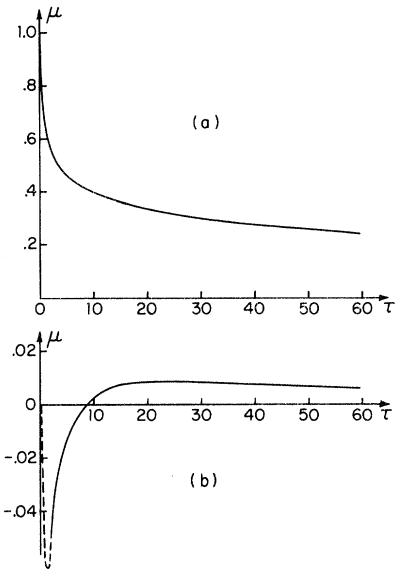

FIG. 3. Function $\mu(\tau)$ for $f_0 = 5.8$ and (a) $x_0 = 0$, (b) $x_0 = 1/\sqrt{3}$. The dashed portion of curve (b) is only schematic because the computer program printed values of μ only at time intervals $\Delta\tau = 2$.

in Fig. 3 for the two cases depicted in Figs. 1 and 2. For $x_0 = 0$, μ decreases monotonically from unity. The instability always shifts toward smaller q, and the tail at large q drops appreciably. For $x_0 = 1/\sqrt{3}$, on the other hand, the first two terms in (6.1) cancel, and the initial instability is dominated by the cubic term as predicted by Cahn.[16] For positive x_0, $\langle y^3 \rangle$ must be negative; thus μ starts at zero, initially goes negative, but quickly changes sign and then stays roughly constant at a small positive value. This value of μ is so small, however, that it has essentially no effect on the S equation. That is, one can simply set $\mu = 0$ in (4.16), which, as far as S is concerned, returns us to Cook's linear fluctuation theory.[15] As seen in Fig. 2, $S(q)$ rises toward the envelope,

$$S(q, \infty) \approx 1/q^2, \quad x_0 = 1/\sqrt{3}. \tag{6.2}$$

In this sense, the system is undergoing critical fluctuations during decomposition near the spinodal. It is only at much later times, when the peak reaches the neighborhood of $\sqrt{\mu} \lesssim 0.1$, that the behavior of μ will become important in (4.16). For the earlier times which we can consider here, it is only the ρ_1 function which gives us an indication that phase separation may be occurring.

As was mentioned in Sec. II, a standard metallurgical analysis of x-ray scattering data involves plotting the quantity

$$\tilde{R}(k^2) \equiv \frac{1}{k^2 \hat{S}} \frac{\partial \hat{S}}{\partial t} \tag{6.3}$$

as a function of k^2 and looking for straight-line behavior of the kind predicted by Eqs. (2.11) and (2.12). In Fig. 4, we have plotted

$$\tilde{\mathcal{R}}(q^2) \equiv \frac{1}{q^2 S} \frac{\partial S}{\partial \tau} \tag{6.4}$$

as a function of q^2 at the times $\tau = 20$ and $\tau = 100$. The results are reminiscent of the experimental data reported in Ref. 7. The curves show no noticeable straight sections, even for values of q in the neighborhood of the peak in $S(q)$. At the peak positions q_p, however, both $\tilde{\mathcal{R}}(q^2)$ curves are very nearly tangent to the lines $\mu - q^2$, as long as μ is chosen here to be the instantaneous $\mu(\tau)$ rather than $\mu(0)$ as required by the linear theory. This last observation suggests that experimental data might usefully be analyzed by looking at such tangent lines, as has, in fact, been done in several cases. (See Figs. 22 and 23 in Ref. 2.) To reinforce this suggestion, we mention that we have also computed $S(q, t)$ for the case $f_0 = 26$, which is appropriate for the alloy Al-Zn according to the thermodynamic data used by deFontaine[27] in his analysis of spinodal decomposition in that system. In this case, although $S(q, t)$ still does not increase exponentially with time, there is a significant straight section in $\tilde{\mathcal{R}}(q^2)$ near q_p. We shall return to the significance of large f_0 in some later comments.

As a further part of our numerical analysis, we have looked at coarsening as a function of time. Wagner,[28] and Lifshitz and Slyozov[29] have predicted that the coarseness of the decomposition will increase like $t^{1/3}$, and this prediction appears to have been verified experimentally in certain cases.[4] On the other hand, the Monte Carlo simulations for kinetic Ising models[9,10] produce much slower behavior. Binder and Stauffer[30] recently have suggested a theoretical coarsening law of the

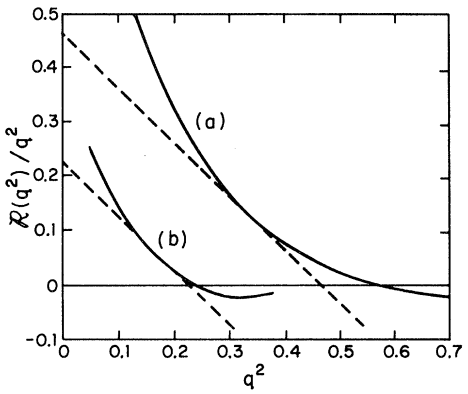

FIG. 4. Reduced amplification factor $\mathcal{R}(q^2)/q^2$ for $f_0 = 5.8$, $x_0 = 0$, and (a) $\tau = 20$, (b) $\tau = 100$. The dashed lines are tangents to these curves at the peak positions $q_p(\tau)$.

form $t^{a'}$, where $a' = 1/(d+3)$ and d is the dimensionality. This prediction seems to be accurately verified in two dimensions.[10] Although there is little reason to believe that our present theory will be valid for coarsening beyond the stage where clusters are two or three correlation lengths in size, it is interesting to note that our data do indicate a slow coarsening with a' appreciably smaller than $\frac{1}{3}$. For the Ising case, $f_0 \cong 5.8$ and $x_0 = 0$, our data are extremely well represented by the function

$$q_p = 1.09\tau^{-a'}, \quad a' = 0.212 \tag{6.5}$$

throughout the interval $4 < \tau < 100$. (We have no results for $\tau > 100$.) Our uncertainty in a' appears to be at most ± 0.005. In the case $f_0 = 26.4$, $x_0 = 0$, we find an even slower coarsening for $\tau \lesssim 50$. Here, a' is roughly $\frac{1}{6}$, perhaps corresponding to a period in which the linear theory is nearly valid and the peak is almost stationary. At $\tau \cong 50$ however, there occurs a break in the $\ln q_p$-vs-$\ln\tau$ curve, and the later coarsening ($50 < \tau < 200$) is again described by $a' \cong 0.21$. Thus, there seems to be some sort of universality of the coarsening predicted by our theory, but, at present, we can offer no way of understanding how this comes about, nor do we know whether the result has any physical significance.

We turn finally to a comparison of our computed structure factor $S(q, \tau)$ with the most recent Monte Carlo data obtained by Marro *et al.*[23] At the time that this report is being written, the only available Monte Carlo data with which we can attempt a meaningful comparison are those for $x_0 = 0$ and $T/T_c = 0.8$. This temperature is quite a bit too low to be in the scaling region, but, as explained in Sec. V, it is very hard to get to long enough times at higher temperatures. For these parameters, the specific conversion factors that we need are

$$\tau = 0.0593t, \quad q = 0.988ka_0. \tag{6.6}$$

We also have

$$S(q, t) = 0.346\hat{S}_M(k, t), \tag{6.7}$$

where $\hat{S}_M$ is the structure factor which has been normalized by Marro *et al.* so that $\hat{S}_M = 1$ at $t = 0$. Note that there are no adjustable parameters whatsoever in these formulas.

In Fig. 5 we show $S(q)$ at five different times τ (solid curves) along with Monte Carlo values (open circles) scaled according to Eqs. (6.6) and (6.7). The crosses in Fig. 5(a) are Monte Carlo points obtained at $T/T_c = 0.91$ and appropriately rescaled. Apart from the fact that our theoretical $S(q)$ lies consistently below the "experimental" values on the high-q side of the peak, the agreement is quite satisfactory. The excellent agreement at small values of q indicates to us that we have not made any serious mistake in our evaluation of the mobility M in Sec. V. What is particularly encouraging is the fact that the position and height of the peak are accurately predicted by our theory all the way out to the latest times for which data is available.

There are at least two possible explanations for the high-q discrepancy. The first is that it is just a departure from scaling, and would go away if we could do the simulation experiments at higher temperatures. The fact that the discrepancy is reduced at $T/T_c = 0.91$, as seen in Fig. 5(a), indicates that this is at least a part of the answer. It is also likely that the missing higher powers of x in $\phi(x)$ are playing some role here. A positive x^6 term in ϕ would tend to increase f_0 via the factor $\phi''(1)$ in Eq. (4.7). This, in turn, would lead to larger values of μ and, thus, larger values of $S(q)$ for large q. These higher powers of x in ϕ must also play an important role in slowing down the growth of the peak in $S(q)$ at late times. This effect shows up, for example, in the Monte Carlo data at $T/T_c = 0.6$, a temperature so low that we must expect strong departures from the scaling version of $\phi(x)$ in the form of large coefficients of x^6, x^8, etc. Here the theoretical $S(q)$ catches up to the "experimental" at about $\tau = 20$ and grows much too rapidly thereafter. At present, we do not know whether this discrepancy can be cured by using a nonscaling ϕ in the formalism developed here, or whether our computational scheme is breaking down in some more serious way. This point is of considerable interest because a very similar late-time discrepancy occurs in trying to fit actual x-ray spectra from the Al-Zn system.[19,27]

VII. CONCLUSIONS

The following general conclusions emerge from the preceding analysis.

(i) The Cahn-Hilliard-Cook linearized theory of spinodal decomposition will be accurate only for very early stages of the decomposition in systems for which the parameter f_0, defined in (4.7), is sufficiently large. Note that, when f_0 becomes infinite, ρ_1 remains sharply peaked in (4.19) and (4.20), and μ remains constant. The simplest way to achieve large f_0 is for the range of interactions to be much larger than the lattice spacing, that is, for the system to be one which is accurately described by mean-field theory. When f_0 is small, as it is for short-range Ising systems, the thermally induced fluctuations are large enough to cause appreciable nonlinear effects even at

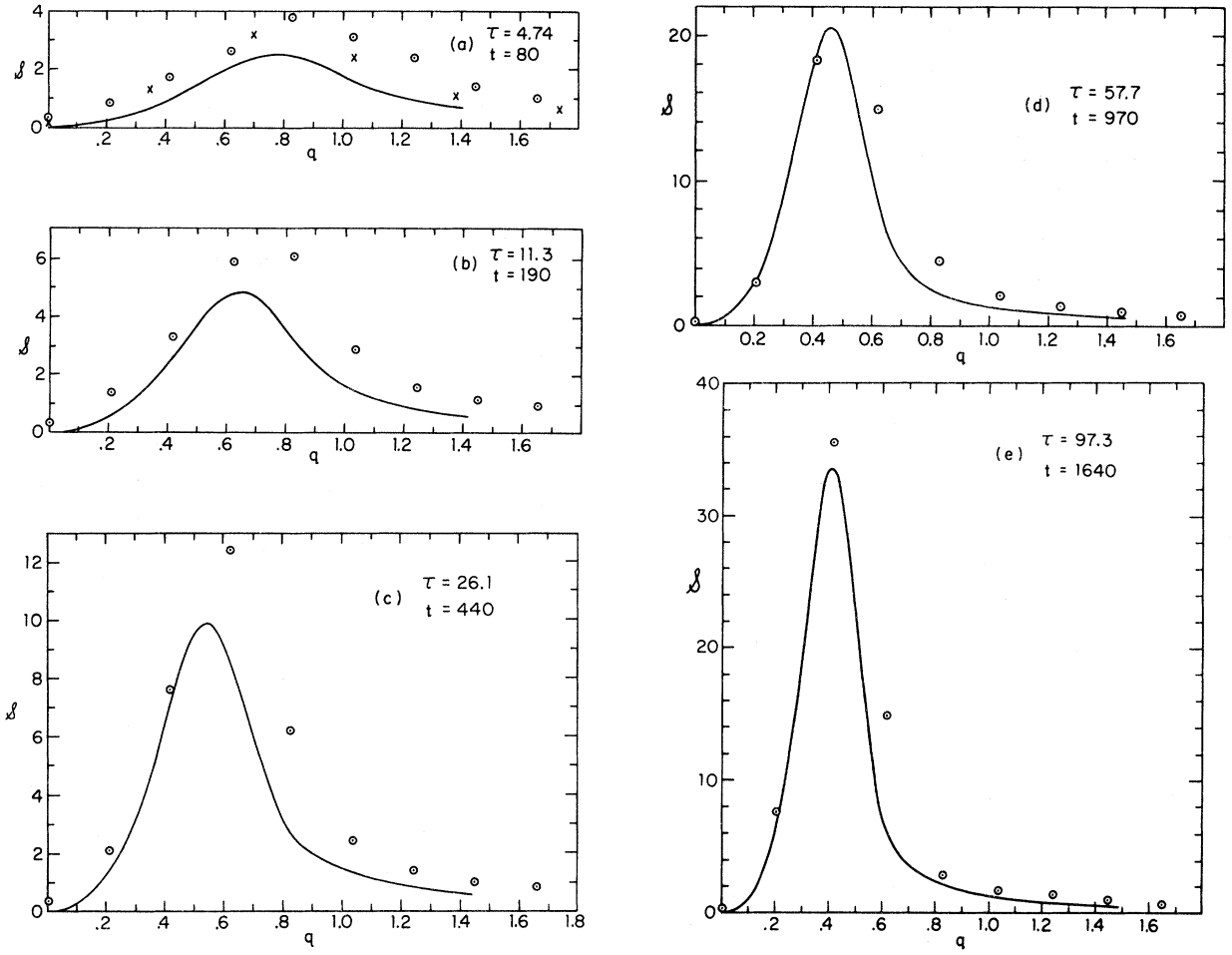

FIG. 5. Graphs of the structure factor $S(q)$ for $f_0 = 5.8$, $x_0 = 0$ at various times τ, shown in comparison with computer simulation of the kinetic Ising model. The solid curves are the results of the present calculations. The circled points are Monte Carlo data obtained on a $30\times30\times30$ lattice at $T/T_c = 0.8$ by Marro *et al.* (Ref. 23). The indicated times t are in units of attempts per site. The crosses in graph (a) denote data obtained at $T/T_c = 0.91$ at time $t = 624$, which corresponds to $\tau = 4.86$ for that temperature.

the earliest stages of the decomposition.

(ii) The position of the peak in the x-ray scattering intensity, $\hat{S}(k)$, is not strongly dependent on the initial composition but is determined, rather, by the range of correlations in the emerging equilibrium phases.

(iii) For decomposition occurring near the center of the spinodal region, the sequence of functions $\hat{S}(k)$ for increasing times after quench will exhibit a sharp, growing peak which moves toward smaller k and displays a crossover phenomenon on the high-k side.

(iv) For decomposition at the spinodal boundary, the sequence of $\hat{S}(k)$ functions will exhibit broader, more slowly growing peaks with no crossover. In this situation, the system will appear to be undergoing critical fluctuations as the phase separation takes place.

(v) Preliminary comparisons of the theoretical results derived here with three dimensional Monte Carlo data show good quantitative agreement for temperatures not too far below T_c. There is some indication, however, that the structure factor may be more sensitive to higher derivatives of the free energy than had been anticipated. On the whole, the present computational scheme does appear to be accurate enough to justify its use in the study of realistic metallurgical systems.

ACKNOWLEDGMENTS

The authors wish to thank Dr. J. Marro, Dr. A. B. Bortz, Dr. M. H. Kalos, and Dr. J. L. Lebowitz for providing results of their Monte Carlo calculations prior to publication. One of the authors (J.S.L.) wishes to thank the Physics Department at Harvard University for its hospitality during the time this work was being completed.

*Research supported in part by AFOSR Grant No. 72-2311 and NSF Grant No. DMR72-02977 A03.

†Permanent address: Carnegie-Mellon University, Pittsburgh, Pa. 15213.

[1]J. W. Cahn, Trans. Metall. Soc. AIME 242, 166 (1968).
[2]J. E. Hilliard, in *Phase Transformations*, edited by H. I. Aronson (American Society for Metals, Metals Park, Ohio, 1970).
[3]K. B. Rundman and J. E. Hilliard, Acta Mettall. 15, 1025 (1967).
[4]E. P. Butler and G. Thomas, Acta Metall. 18, 347 (1970).
[5]G. F. Nielson, Phys. Chem. Glasses 10, 54 (1969).
[6]M. Tomozawa, R. K. MacCrone, and H. Herman, J. Amer. Ceram. Soc. 53, 62 (1970).
[7]N. S. Andreev, G. G. Boiko, and N. A. Bokov, J. Non-Cryst. Solids 5, 41 (1970).
[8]J. S. Huang, W. I. Goldberg, and A. W. Bjerkaas, Phys. Rev. Lett. 32, 921 (1974).
[9]P. Flinn, J. Stat. Phys. 10, 89 (1974).
[10]A. B. Bortz, M. Kalos, J. Lebowitz, and M. Zendejas, Phys. Rev. B 10, 535 (1974).
[11]M. Hillert, D. Sc. thesis (Massachusetts Institute of Technology, 1956) (unpublished).
[12]M. Hillert, Acta Mettall. 9, 525 (1961).
[13]J. W. Cahn, Acta Metall. 9, 795 (1961).
[14]J. W. Cahn, Acta Metall. 10, 179 (1962).
[15]H. E. Cook, Acta Metall. 18, 297 (1970).
[16]J. W. Cahn, Acta Metall. 14, 1685 (1966).
[17]J. S. Langer, Ann. Phys. (N.Y.) 65, 53 (1971).
[18]J. S. Langer and M. Bar-on, Ann. Phys. (N.Y.) 78, 421 (1973).
[19]J. S. Langer, Acta Metall. 21, 1649 (1973).
[20]S. Allen and J. W. Cahn (unpublished).
[21]J. S. Langer, Physica 73, 61 (1974).
[22]M. E. Fisher, Rep. Prog. Phys. 30, 615 (1967).
[23]J. Marro, A. B. Bortz, M. H. Kalos, J. L. Lebowitz (unpublished).
[24]K. Wilson and J. Kogut, Phys. Rep. C 12, 77 (1974).
[25]H. B. Tarko and M. E. Fisher, Phys. Rev. Lett. 31, 926 (1973).
[26]K. Kawasaki, Phys. Rev. 145, 224 (1966); 148, 375 (1966).
[27]D. de Fontaine, Ph.D. thesis (Northwestern University, 1967) (unpublished).
[28]C. Wagner, Z. Elektrochem. 65, 581 (1961).
[29]I. M. Lifshitz and V. V. Slyozov, J. Phys. Chem. Solids 19, 35 (1961).
[30]K. Binder and D. Stauffer, Phys. Rev. Lett. 33, 1006 (1974).